doi:10.1093/brain/awv109 BRAIN 2015: 138; 1894–1906 | 1894

BRAIN
A JOURNAL OF NEUROLOGY

Cortico-pallidal oscillatory connectivity in patients with dystonia

Wolf-Julian Neumann,[1,2] Ashwani Jha,[3] Antje Bock,[1] Julius Huebl,[1] Andreas Horn,[1] Gerd-Helge Schneider,[4] Tillmann H. Sander,[5] Vladimir Litvak[2,*] and Andrea A. Kühn[1,6,7,*]

*These authors contributed equally to this work.

Primary dystonia has been associated with an underlying dysfunction of a wide network of brain regions including the motor cortex, basal ganglia, cerebellum, brainstem and spinal cord. Dystonia can be effectively treated by pallidal deep brain stimulation although the mechanism of this effect is not well understood. Here, we sought to characterize cortico-basal ganglia functional connectivity using a frequency-specific measure of connectivity—coherence. We recorded direct local field potentials from the human pallidum simultaneously with whole head magnetoencephalography to characterize functional connectivity in the cortico-pallidal oscillatory network in nine patients with idiopathic dystonia. Three-dimensional cortico-pallidal coherence images were compared to surrogate images of phase shuffled data across patients to reveal clusters of significant coherence (family-wise error $P < 0.01$, voxel extent 1000). Three frequency-specific, spatially-distinct cortico-pallidal networks have been identified: a pallido-temporal source of theta band (4–8 Hz) coherence, a pallido-cerebellar source of alpha band (7–13 Hz) coherence and a cortico-pallidal source of beta band (13–30 Hz) coherence over sensorimotor areas. Granger-based directionality analysis revealed directional coupling with the pallidal local field potentials leading in the theta and alpha band and the magnetoencephalographic cortical source leading in the beta band. The degree of pallido-cerebellar coupling showed an inverse correlation with dystonic symptom severity. Our data extend previous findings in patients with Parkinson's disease describing motor cortex-basal ganglia oscillatory connectivity in the beta band to patients with dystonia. Source coherence analysis revealed two additional frequency-specific networks involving the temporal cortex and the cerebellum. Pallido-cerebellar oscillatory connectivity and its association with dystonic symptoms provides further confirmation of cerebellar involvement in dystonia that has been recently reported using functional magnetic resonance imaging and fibre tracking.

1 Department of Neurology, Campus Virchow Klinikum, Charité–University Medicine Berlin, Augustenburger Platz 1, 13353 Berlin, Germany
2 The Wellcome Trust Centre for Neuroimaging, UCL Institute of Neurology, 12 Queen Square, London WC1N 3BG, UK
3 Sobell Department of Movement Disorders, UCL Institute of Neurology, Queen Square, London WC1N 3BG, UK
4 Department of Neurosurgery, Campus Virchow Klinikum, Charité–University Medicine Berlin, Augustenburger Platz 1, 13353 Berlin, Germany
5 Physikalisch–Technische Bundesanstalt, Institut Berlin, Abbestr. 2-12, 10587 Berlin, Germany
6 Berlin School of Mind and Brain, Charité - University Medicine Berlin, Unter den Linden 6, 10099 Berlin, Germany Berlin, Germany
7 NeuroCure, Charité - University Medicine Berlin, Charitéplatz 1, 10117 Berlin, Germany

Correspondence to: Prof. Dr. Andrea A. Kühn,
Department of Neurology, Charité,
University Medicine Berlin,
Campus Virchow Klinikum,
Augustenburger Platz 1,
13353 Berlin, Germany

Received December 2, 2014. Revised February 10, 2015. Accepted February 26, 2015. Advance Access publication May 2, 2015

E-mail: andrea.kuehn@charite.de

Keywords: globus pallidus internus; oscillations; dystonia; magnetoencephalography; deep brain stimulation

Abbreviations: DBS = deep brain stimulation; GPi = globus pallidus internus; LFP = local field potential; MEG = magnetoencephalography; SPM = statistical parametric mapping; TWSTRS = Toronto Western Spasmodic Torticollis Rating Scale

Introduction

The dystonias are a heterogeneous group of syndromes that are characterized by involuntary twisting movements and abnormal posturing, sometimes with associated tremor (Fahn, 1988). Early neuropathological, CT and MRI studies investigating the pathophysiological mechanisms underlying this movement disorder have suggested that basal ganglia dysfunction plays a central role (Hallett, 2006). More recently, abnormal activity in a wider network of regions has been identified including the cortex, cerebellum, brainstem and spinal cord (Hendrix and Vitek, 2012). Both at rest and during voluntary movements, neuroimaging studies have demonstrated abnormal activation patterns in the putamen, pallidum, thalamus, cerebellum and motor and premotor cortices (Ceballos-Baumann *et al.*, 1995; Eidelberg *et al.*, 1998; Kumar *et al.*, 1999; Detante *et al.*, 2004; Lehericy *et al.*, 2013). Electrophysiological evaluations of the sensorimotor and premotor cortices have suggested that there is a loss of intracortical inhibition, increased cortical plasticity and abnormal sensorimotor integration in patients with dystonia (Vidailhet *et al.*, 2009; Quartarone and Hallett, 2013). Deep sites such as the basal ganglia have traditionally been difficult to electrophysiologically access in humans. Deep brain stimulation surgery for movement disorders now affords the opportunity to record from macroelectrodes in these areas via surgically placed deep brain stimulation (DBS) electrodes, before electrical stimulation (Brown and Williams, 2005). Such recordings from the target areas of DBS have revealed that subjects with Parkinson's disease have a characteristic increase in local beta frequency activity whilst subjects with dystonia have increased lower frequency activity (Silberstein *et al.*, 2003; Liu *et al.*, 2008). Furthermore, pallidal low frequency oscillations temporally lead similar oscillations in dystonic muscle activity, suggesting that they may play a causal role (Sharott *et al.*, 2008).

DBS of the globus pallidus internus (GPi) is a successful treatment for patients with generalized, segmental and cervical dystonia refractory to medical therapy (Vidailhet *et al.*, 2005, 2007; Kupsch *et al.*, 2006; Ostrem and Starr, 2008; Volkmann *et al.*, 2012, 2014). However, the therapeutic mechanism of DBS in dystonia is still not fully understood. One proposed hypothesis is that DBS suppresses or overrides the aforementioned pathological oscillatory network activity within cortico-basal ganglia circuits (Hammond *et al.*, 2007; Brown and Eusebio, 2008; McIntyre and Hahn, 2010; Hendrix and Vitek, 2012). However, less is known about the wider network implications of such activity, in particular the physiological and pathological oscillatory activity 'between' distant brain regions, in patients with dystonia. A novel technique that records subcortical local field potentials (LFPs) from DBS electrodes and simultaneous cortical whole head magnetoencephalography (MEG) has made it possible to electrophysiologically characterize the cortico-basal ganglia network in subjects with Parkinson's disease using coherence measures to characterize functional connectivity (Litvak *et al.*, 2010, 2011*a*). Coherence describes the spectral distribution of oscillatory synchronization between concurrent signals and can be interpreted as interaction or communication between brain areas. Two spectrally and spatially distinct oscillatory networks were found in patients with Parkinson's disease at rest involving the subthalamic nucleus and cortical sources: a frontal motor network for the beta band and a predominantly temporal network for the alpha band, which were modulated during movement and tremor episodes (Hirschmann *et al.*, 2011, 2013; Litvak *et al.*, 2011*a*, 2012; Oswal *et al.*, 2013).

The aim of the present study was to use this novel technique of simultaneous MEG-LFP recording to investigate patterns of cortico-pallidal oscillatory connectivity in patients with dystonia. We hypothesized that such networks would again be spatially and spectrally segregated in dystonic patients but that key spatial and/or spectral features would be distinct from the abnormalities found in Parkinson's disease and that such features would provide new insights into the brain networks involved into the pathophysiology of dystonia.

Materials and methods

Patients and surgery

Nine patients [six females; age 50.1 ± 3.9 years, range 24–68 years; disease duration 12.8 ± 2.5 years, range 3–23 years; mean ± standard error of the mean (SEM)] with either segmental dystonia ($n = 2$; Cases 2 and 5), cervical dystonia ($n = 5$; Cases 3, 4, 6, 7 and 8) or generalized dystonia ($n = 2$; Cases 1 and 9) who underwent bilateral implantation of DBS electrodes in the GPi were included in the study. All patients participated with informed consent and with the agreement of the ethical committee of the Charité–Universitätsmedizin, Berlin, Campus Virchow-Klinikum. The study was conducted according to the Declaration of Helsinki. Clinical details are summarized in Table 1. The DBS macroelectrode used was model 3389 (Medtronic) with four platinum-iridium

cylindrical surfaces of diameter 1.27 mm, length 1.5 mm and centre-to-centre separations of 2 mm. Contacts 0 and 3 were the lowermost and uppermost contacts, respectively. Correct placement of the DBS electrodes was guided by intraoperative microelectrode recordings and confirmed by postoperative MRI. Postoperative 3D electrode localization was conducted using the Lead-DBS toolbox (Horn and Kühn, 2014; see Fig. 1 for an example). In brief, preoperative and postoperative magnetic resonance images were fused and normalized to Montreal Neurological Institute (MNI) space, before mapping the contacts to normalized subcortical atlases (BGHAT atlas, Prodoehl *et al.*, 2008; Harvard-Oxford subcortical/cortical atlas, Frazier *et al.*, 2005). This confirmed that 51/54 contact pairs had at least one contact in the internal pallidum, with the remaining three contact pairs from two patients (Case 2: R01, Case 7: R01/L01) lying below the edge of the target.

Experiments and recordings

Simultaneous 125 channel MEG (YOKOGAWA ET 160) and pallidal LFP recordings were conducted 1 to 7 days after DBS electrode implantation (mean ± SEM = 3 ± 0.37 days), while the DBS leads were externalized. Rest recordings of 3–4 min were conducted, during which the patients were lying still with eyes open and instructed not to move. To avoid movement artefacts, patients with severe phasic head movements or head tremor were not included in the study. All data were recorded at a sampling rate of 2000 Hz. Electro-oculographic, EMG and LFP recordings were recorded simultaneously through the integrated EEG system. Recordings from four DBS electrode contacts were referenced to contact 0 of the left electrode and later re-referenced offline (see below).

Data analysis

Statistical parametric mapping (SPM; Litvak *et al.*, 2011*b*) (http://www.fil.ion.ucl.ac.uk/spm/), Fieldtrip (Oostenveld *et al.*, 2011) (http://www.ru.nl/neuroimaging/fieldtrip/) and Data Analysis in Source Space (DAiSS, https://code.google.com/p/spm-beamforming-toolbox/) toolboxes were used. To limit the effects of volume conduction to distant sources, LFP recordings were re-referenced to a bipolar montage between adjacent contact pairs (01, 12, 23). To avoid selection bias, all three contact pairs (01, 12, 23) from the DBS electrodes of all patients were included in the analysis. The data were then down-sampled to 300 Hz. High-pass (>1 Hz) and notch filters (at 50, 100 and 150 Hz) were applied to limit effects of line noise (fifth order zero-phase Butterworth filters). Continuous rest recordings were divided into arbitrary epochs of 3.41-s length (1024 samples). Epochs were rejected from further analysis if they contained artefacts in either MEG or LFP data. Artefacts in the LFP recordings were identified by thresholding the LFP amplitude at 30 μV (Litvak *et al.*, 2011*a*). This threshold was set by examining the typical values for clean data and artefactual deflections across epochs and subjects. The MEG data were contaminated by artefacts generated by ferromagnetic percutaneous connection wires. It was previously shown (Litvak *et al.*, 2010) that such artefacts can be suppressed by beamforming. However, the Yokogawa system used in the present study has a lower dynamic range than the CTF-MEG system used previously, resulting in intermittent saturations in some of the channels close to the wires. These

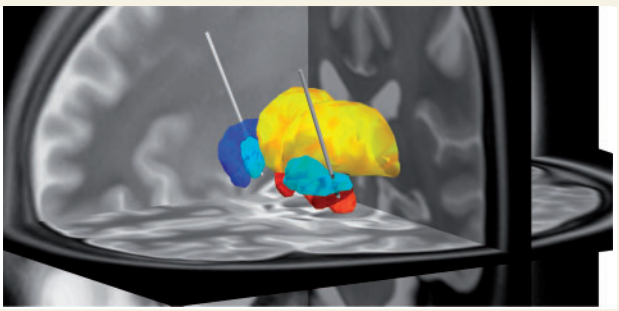

Figure 1 Deep brain stimulation electrode location. Example of a 3D reconstruction of a DBS lead for electrode localization, with contacts in the internal pallidum (light blue structure; Case 4). The thalamus (yellow), external pallidum (dark blue), subthalamic nucleus (dark red) and red nucleus (light red) are visualized for better orientation.

Table 1 Clinical details of the patients

Case	Age	Sex	Diagnosis	TWSTRS	BFMDRS	Disease duration	*n* excluded sensors	Theta peak location (mm *x y z* MNI)	Alpha peak location (mm *x y z* MNI)	Beta peak location (mm *x y z* MNI)
1	48	F	Generalized dystonia	na	16	20	1/125	54 −24 6	−2 −50 −48	40 −2 34
2	55	M	Segmental dystonia[b]	20	na	12	0/125	32 −28 −28	2 −48 −48	4 −46 64
3	51	F	Cervical dystonia	23	na	3	20/125	56 −44 −16	24 −64 −46	14 −8 70
4	52	F	Cervical dystonia	22	na	11	14/125	46 −14 −22	0 −72 −42	48 −4 28
5	48	F	Segmental dystonia[c]	25	na	6	15/125	54 −32 −18	16 −84 −16	46 −30 52
6[a]	68	M	Cervical dystonia	16	na	23	86/125	na	na	na
7	47	F	Cervical dystonia	15	na	4	18/125	30 −32 −28	0 −52 −40	32 −10 54
8	58	M	Cervical dystonia	18	na	20	26/125	56 −32 6	8 −62 −40	4 −2 70
9	24	F	Generalized dystonia (DYT 1)	na	27	16	0/125	no peak	38 −78 −34	36 −2 54

Note that the TWSTRS was used to assess symptom severity in patients with clinical features involving primarily the neck, whereas the Burke Fahn Marsden Dystonia Rating Scale (BFMDRS) was used for the patients with generalized dystonia. [a]This case was excluded from the analysis due to artefacts. [b]Case 2 had cervical dystonia with additional postural hand tremor. [c]Case 5 had cervical dystonia with mild contraction of the right abdominal wall.

saturated segments were defined as segments where the differences between adjacent samples stayed <5 fT for 10 consecutive samples or more. Epochs with amplitude jumps of >10 pT between consecutive samples were also excluded. If for a particular MEG channel $>20\%$ of the epochs were contaminated by these artefacts, the channel was excluded from further analysis (see Table 1 for details). In one patient (Case 6), metal artefacts led to exclusion of 86/125 sensors; thus, data from this patient were omitted from further analysis. The mean number of excluded channels was 13 (range 0–26), concentrated in the area of the percutaneous connection wires on the left hemisphere (location corresponding to the area around electrode F3 in the 10-20 EEG system). After artefact rejection, a mean ± SEM of 216.9 ± 16.2 s (range 133–293 s) were analysed, resulting in an average of 62.9 ± 5.25 SEM trials (range 39–75 trials) in eight remaining patients. All data were visually inspected before and after automatic artefact rejection.

Characterization of the frequency distribution of significant LFP-MEG coherence

The principal correlate of functional connectivity investigated in this study was coherence, which provides a frequency domain measure of the linear phase and amplitude relationships between signals (Buzsaki and Draguhn, 2004; Litvak *et al.*, 2010). Single-subject analysis at the sensor level was designed to investigate the frequency distribution of significant peaks of coherence before group analysis. We used the procedure originally suggested by Litvak *et al.* (2011*a*). MEG and bipolar GPi-LFP epoched data were converted to the frequency domain (range 5–45 Hz with a frequency resolution of 2.5 Hz, and 55–95 Hz with frequency resolution of 7.5 Hz) using the multi-taper method (Thomson, 1982). Coherence was then calculated between each GPi-LFP channel and each MEG channel. Scalp maps of coherence for each frequency bin were linearly interpolated to produce a 2D image (64 × 64 pixels). The resulting images were stacked to produce a 3D image with two spatial and one frequency dimension. Thus, 3D images for the low and high frequency ranges were created for each LFP channel in each patient. Significant regions of coherence within these images were determined by statistical comparison to 10 surrogate coherence images in which any coherence was destroyed. The surrogate coherence images were generated from the same MEG trials, but with the order of GPi-LFP trials shuffled. To ensure conformance to the assumptions of random field theory, all images were smoothed with a Gaussian kernel (10 mm × 10 mm × 2.5 Hz for low frequency, and 10 mm × 10 mm × 7.5 Hz for high frequency images). Standard SPM procedures were used for a two-sample *t*-test between the original image and the 10 surrogate images with a family-wise-error corrected threshold of $P < 0.01$ to identify significant regions in sensor space and frequency. For each original LFP-MEG coherence image in each patient, frequencies of the clusters of significant coherence were identified and taken into a histogram (Fig. 2B) to visualize the frequency distribution of significant sensor level coherence across patients.

Characterization of coherent source activity across patients

To identify the spatial topography and spectral properties of distinct frequency-specific cortico-pallidal coherence networks, we used MEG beamforming. For this method, a linear projection of sensor data is generated by using a spatial filter computed from the lead field of the source of interest and the data covariance in the time domain (Van Veen *et al.*, 1997) or the cross-spectral density matrix in the frequency domain (Gross *et al.*, 2001). For lead field computation, a perturbed sphere forward model (Nolte, 2003) was created based on an inner skull mesh obtained by inverse-normalizing a canonical mesh to the subject's individual preoperative MRI image (Mattout *et al.*, 2007). All MEG data sets were coregistered to the individual patient's MRI by using MEG head position indicator coils attached to the nasion and left and right pre-auricular points. The DICS (dynamic imaging of coherent sources) beamforming method was used to locate cortical sources coherent to the GPi-LFP activity (Gross *et al.*, 2001). The coherence values were computed on a 3D grid in Montreal Neurological Institute space, with spacing of 5 mm bounded by the inner skull surface. Values at the grid points were then linearly interpolated to produce volumetric images with 2 mm resolution. The images were stored in Neuroimaging Informatics Technology Initiative (NIfTI) format and smoothed with an 8 mm isotropic Gaussian kernel. The resulting 3D images of LFP-MEG coherence were compared to surrogate images from phase shifted data using SPM procedures (Friston *et al.*, 1994; Litvak *et al.*, 2011*b*). Original and surrogate coherence images were created for five frequency bands, theta (4–8 Hz), alpha (7–13 Hz), beta (13–30 Hz), low gamma (30–60 Hz) and high gamma (60–90 Hz) and taken into the analysis. Images derived from the left pallidal electrodes were reflected across the median sagittal plane, to allow comparison of sources ipsilateral and contralateral to the GPi regardless of the original hemisphere. All images were subjected to a fixed-effect ANOVA to test for a significant difference between real and surrogate coherence images, with subject and side as additional factors. A family-wise error (FWE) corrected threshold of $P < 0.01$ and a minimum voxel extent of 1000 voxels were chosen to identify significant regions of cortico-pallidal coherence. The MNI coordinates of the global maxima for each significant frequency band on the group level were further used for single patient analysis and source extraction. Single patient peak locations were analysed from averaged DICS images from all contact pairs by identifying local maxima in proximity to the group peak. Virtual electrode signals were extracted from group coherence peaks for each frequency band using a linearly constrained minimum variance beamformer (Van Veen *et al.*, 1997) and regularization set at 0.01% of the mean of the diagonal of the channel covariance matrix (Litvak *et al.*, 2010). Source and GPi-LFP power and coherence estimates were calculated from the resulting extracted source channels and are presented as the mean across all pallidal contact-pairs and patients. Individual peaks of GPi-LFP power spectra were investigated visually and reported. To investigate the effective directionality of functional coupling between the cortical sources and the pallidal LFP signal, we used a non-parametric variant of Granger causality (Brovelli *et al.*, 2004) averaged for each frequency band. To identify

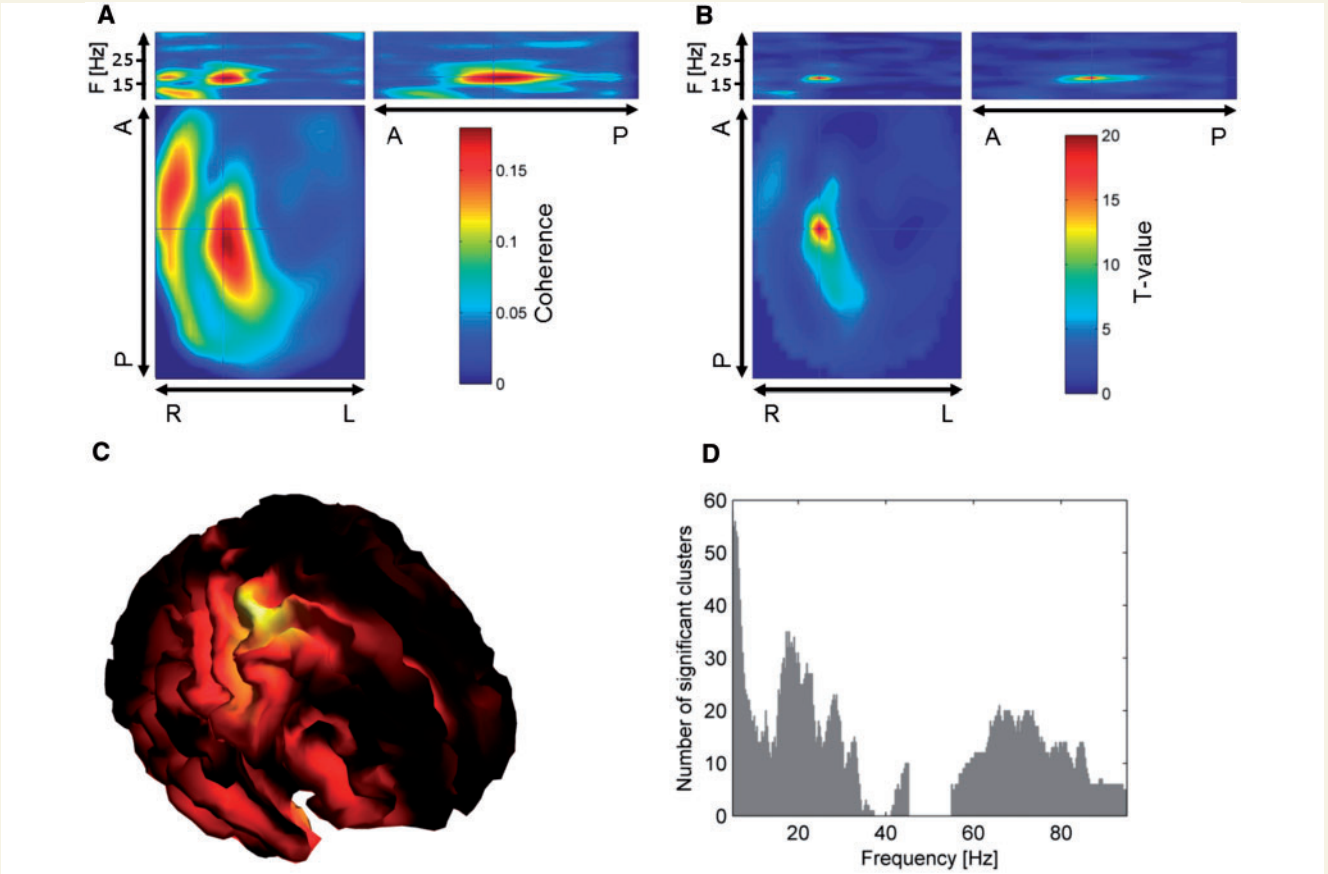

Figure 2 Sensor space analysis. Representative pallidal LFP-MEG sensor coherence map (**A**, the colour axis represents coherence) for the low frequency band with the corresponding SPM T-statistic (**B**, the colour represents T-values for each point on the 3D sensor map) and the corresponding source analysis (**C**) localized to the ipsilateral motor cortex (Area 6) for one GPi contact pair (Case 4 contact pair R12). The upper plots (A and B) show the spatial dimension (left-right and anterior-posterior) on the *x*-axis with frequency on the *y*-axis (5–45 Hz). The large figures on the lower left (A and B) show the two spatial dimensions at the frequency of the peak (18 Hz). The crosshair in A and B is centred on the highest T-value of the peak. The histogram (**D**) of all significant coherence clusters from the individual sensor space analyses visualizes the number of significant peaks in individual patients regardless of the sensor location. A widespread distribution of significant coherence peaks can be seen, predominantly in the 5 to 35 Hz and 60 to 85 Hz range. A = anterior; F = frequency; L = left; P = posterior; R = right.

significant directional coupling, original data were compared to time-reversed data (Haufe *et al.*, 2013) across all patients for each extracted source in the defined frequency range using right-tailed paired *t*-tests. This procedure has proven to suppress the influence of weak data asymmetries not related to time-lagged interactions in the data, while it is statistically powerful in the detection of meaningful strong asymmetries (Haufe *et al.*, 2013). Hence, in the case of true directional interaction a significantly higher Granger causality value is expected for the original signals compared to the reversed surrogate. Therefore, it was tested whether the results were significantly greater across the group for the original data when compared to the reversed surrogate data.

Correlation with clinical symptoms

To investigate a potential relation of LFP–source coherence and dystonic symptom severity, the preoperative Torticollis severity scale that is part of the Toronto Western Spasmodic Torticollis Rating Scale (TWSTRS) was documented for patients with cervical or segmental dystonia (all analysed patients, apart from Cases 1 and 9). Note that patients with segmental dystonia had mild additional symptoms that were not covered by the TWSTRS (Case 2: postural hand tremor; Case 5: contraction of the right abdominal wall). Non-parametric Spearman's correlations were used to investigate a potential association of the TWSTRS severity score and the coherence value in the contact pair, with the highest averaged frequency band LFP-MEG coherence for the temporal theta (4–8 Hz), cerebellar alpha (7–13 Hz) and motor-cortical beta band (13–30 Hz) source.

Results

Spectral distribution of cortico-pallidal coherence

Significant peaks of cortico-pallidal coherence were present in all patients at the sensor level. An example of sensor level coherence with a significant beta peak and the resulting source coherence on an individual patients' cortical mesh is shown in Fig. 2. Frequencies of peaks were

spread across the 5–95 Hz spectrum, with a concentration in the beta range (13–30 Hz; Fig. 2D).

Spatial distribution of frequency-specific cortico-pallidal coherence

Topographical mapping of LFP-MEG coherence revealed frequency-specific pallidal connectivity to sensorimotor cortical areas, temporal areas and the cerebellum. The coherence patterns were clearly lateralized to the ipsilateral hemisphere. For each frequency band, DICS images with their corresponding surrogate phase shifted DICS pairs (96 images from 48 contact pairs from 16 hemispheres from eight patients) were subjected to a fixed-effect ANOVA with subject and side as additional factors. Three significant clusters of cortico-pallidal coherence were revealed, in the theta (4–8 Hz), alpha (7–13 Hz) and beta (13–30 Hz) bands. The results are presented in Fig. 3.

In the theta band, a cluster extending from subcortical areas to the temporal cortex, with the coherence maximum in the inferior temporal gyrus, was identified ($t = 8.87$; $P < 0.0001$; cluster size: 4424; MNI coordinates $x = 44$, $y = -26$, $z = -17$). A cluster restricted to the central cerebellum was significant in the alpha band ($t = 6.18$; $P < 0.0001$; cluster size: 6688; MNI coordinates $x = 2$, $y = -32$, $z = 13$). This cluster overlapped peripherally with the brainstem. However, this overlap vanished when a more conservative FWE corrected P-value threshold ($P < 0.00001$) was chosen. In line with a role of beta oscillations in the sensorimotor network, cortico-pallidal coherence in the beta band (13–30 Hz) was significant in the sensorimotor areas ($t = 8.09$; $P < 0.0001$; cluster size: 24669; MNI coordinates $x = 30$, $y = -14$, $z = 57$).

For the low gamma band (30–60 Hz) a sensorimotor region and two subcortical clusters, and for the high gamma band (60–90 Hz) a small subcortical cluster reached significance ($P < 0.05$ FWE corrected), but did not survive our stringent thresholding criteria and were therefore not further analysed.

All other clusters remained significant, when the three contact pairs that were off target in the postoperative imaging were excluded. A direct comparison of hemispheres (left versus right) did not reveal significant differences in any of the frequency bands. Analysis of individual source locations confirmed the consistency of our findings in individuals within the patient group (Fig. 4). In the theta band, 7/8 patients had a local peak within an average distance of 19.07 ± 2.17 mm from the group mean in MNI space. Similar distances were found for the alpha (8/8 patients, mean distance ± SEM 21.38 ± 5.90 mm) and beta bands (8/8, 25.05 ± 4.16 mm).

Cortical and pallidal spectral power, coherence and directionality of information flow

In each subject, using a linearly constrained minimum variance beamformer, virtual channels of cortical activity were extracted from the locations of maximum coherence (group peak) in the significant clusters for each frequency band. Figure 5 shows the power spectra, LFP-source coherence and directionality measures for each of the three extracted sources. The cortical power spectra showed distinct low frequency peaks at ~10 Hz (including theta and alpha band) and additional increased power in the frequency range up to ~20 Hz for the motor cortical beta band source. For the pallidal LFP signals, power-spectra were averaged across all contact pairs and all patients for visualization. On an individual level, all patients had distinct low frequency peaks in 30/44 contact pairs overall (range 7–12 Hz; mean ± SEM 9 ± 0.5 Hz). A clear spectral

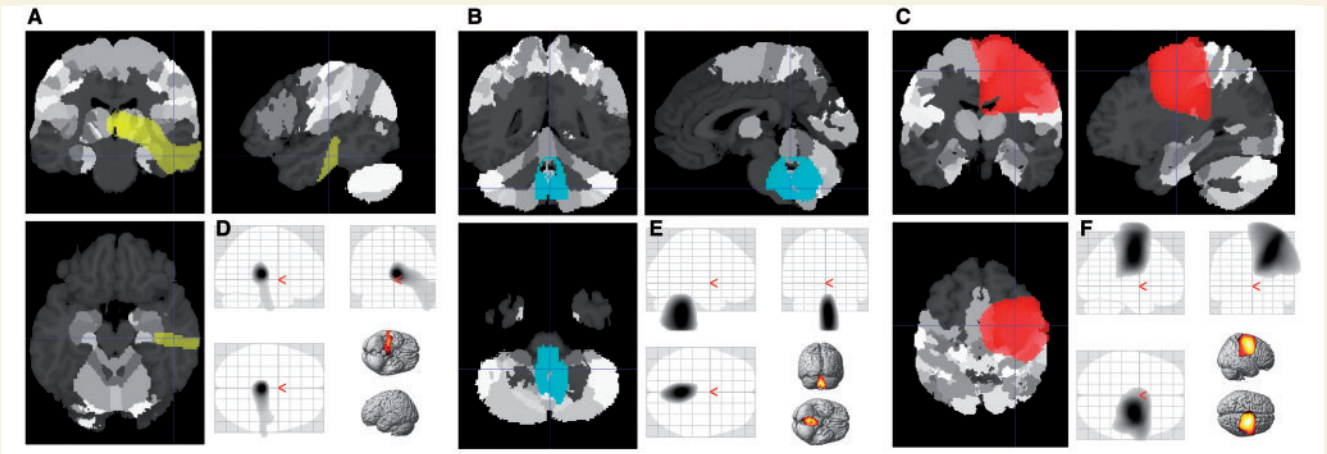

Figure 3 Across group source analysis. SPM analysis of source coherence across the group revealed three distinct networks of LFP-MEG coherence. A mid-temporal theta network (**A**), a cerebellar alpha network (**B**) and a sensorimotor beta network (**C**). Coloured 3D images represent coherence (**A–C**) and are centred to the global maximum within the significant localization and masked for visualization as described in the methods section. Black and white SPM images (**D–F**) represent the corresponding significant voxels from the SPM ANOVA.

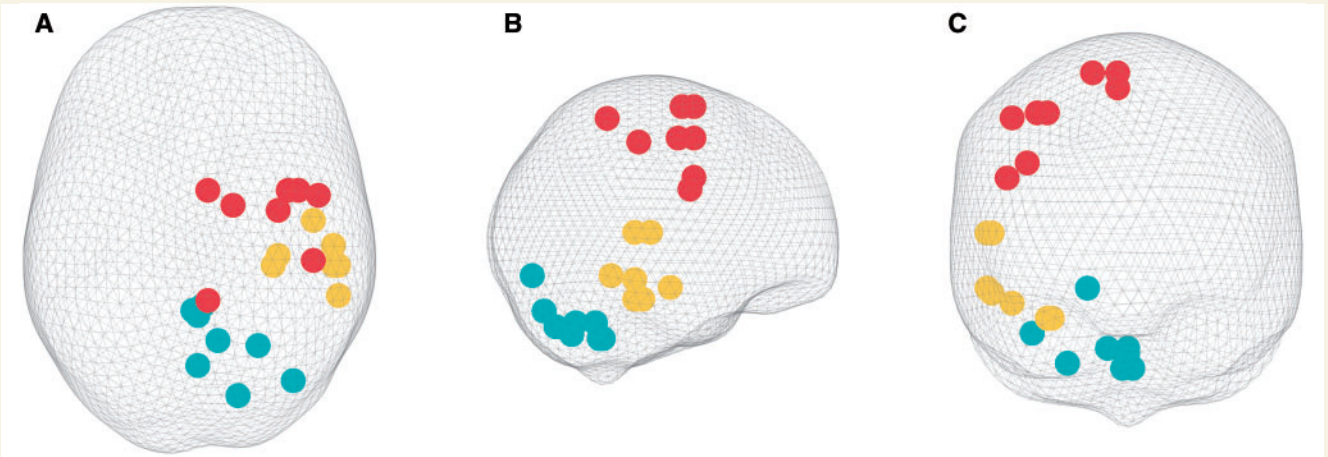

Figure 4 Individual peak localization. Locations of individual local maxima closest to the respective group peak for the theta (yellow), alpha (blue) and beta band (red) were identified in the averaged source coherence images across all contact-pairs for each patient and projected to 'glass brains' (inner boundary of skull marked with grey mesh) viewed from the above (**A**), right (**B**) and front (**C**). All images from left hemispherical contact-pairs were mirrored along the sagittal plane prior to averaging.

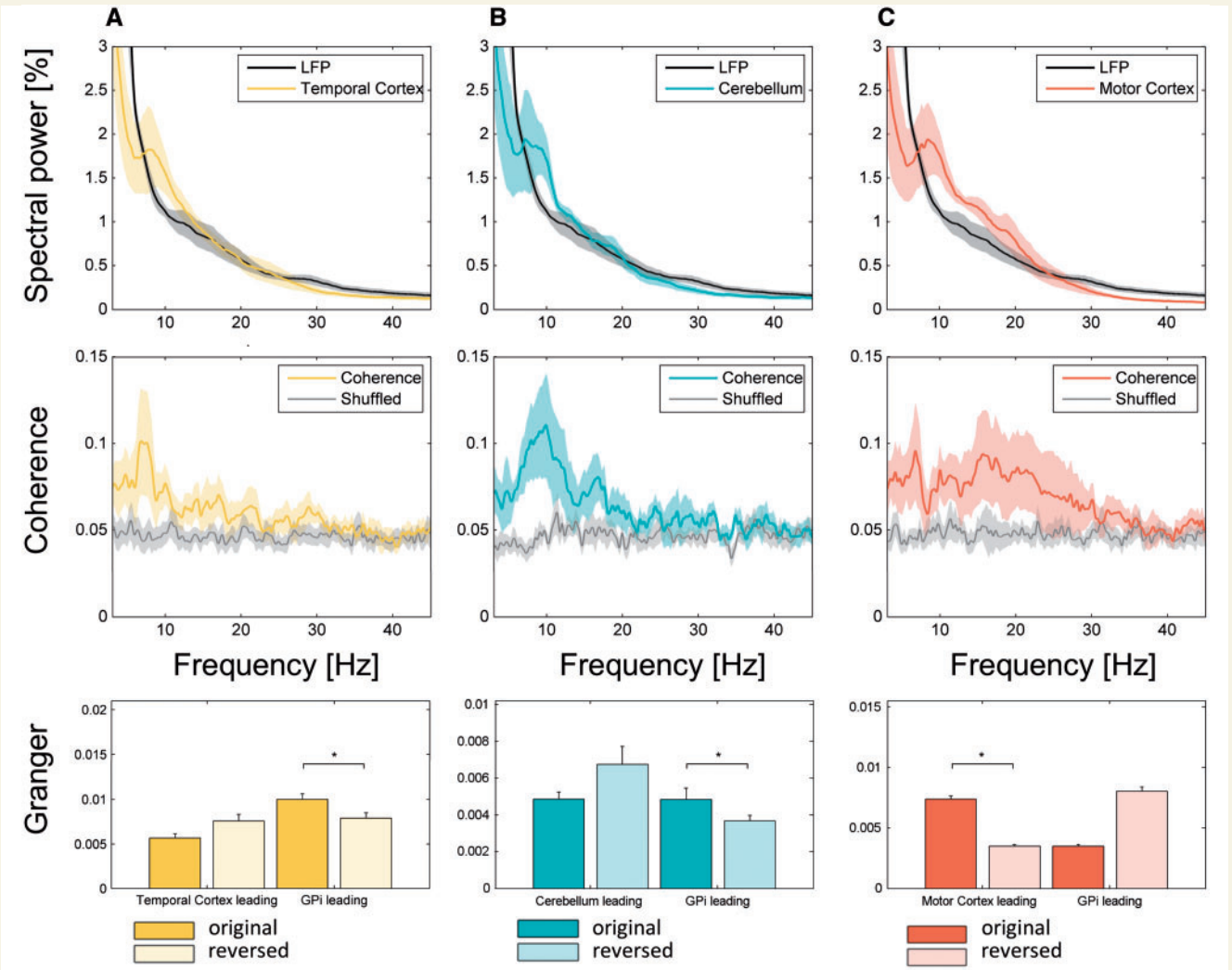

Figure 5 Source extraction and directionality analysis. Linearly constrained minimum variance beamformer (LCMV) source extraction allowed power, coherence and directionality analysis of the significant sources. The top first row shows the averaged power spectra and the second row the coherence spectra for the temporal theta (**A**), the cerebellar alpha (**B**) and the motor cortical beta (**C**) sources. The lowermost row shows the averaged Granger causality measure for the respective frequency bands [4–8 Hz (**A**), 7–13 Hz (**B**), 13–30 Hz (**C**)] of the three identified sources in comparison to reversed data. *$P < 0.05$ **$P < 0.001$.

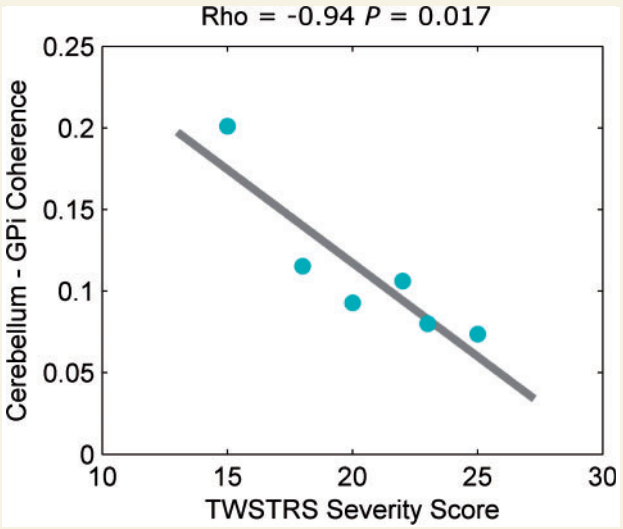

Figure 6 Inverse correlation of pallido-cerebellar coupling and dystonic symptom severity. Spearman's correlation between pallido-cerebellar alpha band coherence and dystonic symptom severity as measured by the TWSTRS severity scale revealed an inverse relationship (Spearman's Rho = −0.94, $P = 0.017$).

distribution of LFP-MEG coherence was found for each cluster, with a focal theta peak (4–7 Hz) for the temporal cortex, a broader alpha band peak (6–13 Hz) for the cerebellar source, and two peaks for the motor cortical source (4–8 Hz + 10–30 Hz). Directionality analysis for the relevant frequency bands for each source revealed that the GPi drove the temporal cortex in the theta range (4–8 Hz; $P < 0.01$) and the cerebellum in the alpha range (7–13 Hz; $P = 0.01$). The motor cortical source drove the GPi in the beta range ($P < 0.001$). Beta band activity in the pallidum has previously shown to be driven by the motor cortex in LFP-EEG studies (Williams *et al.*, 2002) and similar results were found for LFP-MEG and LFP-EEG coherence from the subthalamic nucleus in patients with Parkinson's disease (Litvak *et al.*, 2011*a*).

Correlation of cortico-pallidal coherence and dystonic symptom severity

A negative correlation was found between the degree of pallido-cerebellar connectivity and clinical symptom severity as measured by the TWSTRS. Averaged pallido-cerebellar alpha band coherence (7–13 Hz) negatively correlated with the preoperative TWSTRS score in patients with segmental or cervical dystonia ($n = 6$, Rho = −0.94, $P = 0.017$; Fig. 6), meaning that higher connectivity values were associated with less prominent dystonic motor symptoms in our patients. Detailed analysis revealed that higher scores due to additional symptoms in segmental dystonia patients (not covered in the TWSTRS) would improve (Case 2) or not change (Case 5) the rank based Spearman correlation. No significant correlation was found for the motor cortical beta and theta as well as the temporal theta source (Supplementary Fig. 1).

Discussion

We have demonstrated that the human internal pallidum is interconnected with the cerebral cortex in spatially and spectrally distinct functional oscillatory networks in patients with idiopathic dystonia. Three network connections with the pallidum were identified. Theta band coherence was identified with the temporal cortex, an alpha band coherence with a central cerebellar source, and the beta band coherence with motor and premotor cortical regions. Interestingly, the amount of coupling in the alpha band between the internal pallidum and the cerebellum was inversely correlated with the patients' preoperative clinical state as measured by the TWSTRS. Although correlation does not prove causation, the demonstration of a significant correlation between cerebello-pallidal alpha band coherence and dystonic symptom severity suggests a pathophysiological role for alpha band oscillatory network activity in dystonia.

Before we proceed with a more detailed discussion of our findings, we should consider the potential limitations of our study. The methodological effort, combined with the sparseness of dystonic DBS patients suited for MEG recordings, led to a relatively small and heterogeneous cohort of patients; we tried to compensate for this by introducing conservative statistical thresholds and thorough validation of individual results, both in sensor and in source space. In this regard, it should be noted that the cerebellar alpha band group peak overlaps partially with the brainstem. This is of interest, because brainstem lesions can cause dystonic symptoms (Vidailhet *et al.*, 1999) and altered structural basal ganglia–brainstem connectivity has been reported in dystonia (Blood *et al.*, 2012). Thus, the observed alpha band coherence could be partially originated from the brainstem. However, the facts that all patients had the local maxima in the cerebellum and not in the brainstem, and that an even more conservative statistical threshold confined the source of alpha band coherence to the cerebellum, favours the cerebellum as the relevant source of coupling. Further, magnetic artefacts led to an exclusion of some of the channels near the DBS lead externalization in the left hemisphere, which may have compromised the reliability of coherence measures in this area. A potential influence of this channel exclusion on our results cannot be ruled out; however, no hemispherical differences in coherence patterns were revealed by the statistical analysis. Next, the correlation of alpha band coherence and clinical symptoms are obtained by investigating the severity of predominant cervical dystonic symptoms and we should be cautious not to generalize the findings to all forms of dystonia. Moreover, an inherent limitation of intracranial recordings in humans is the lack of healthy controls. Hence, we cannot predict the

pathophysiological influence of the disease on the reported networks, as our group consisted of patients with different types of dystonia with partially persistent motor symptoms at rest. With the intent to discuss the functional roles of the networks, we should note that the demonstrated results are derived without any functional modulation, and more likely reflect a resting or default mode network (Laufs *et al.*, 2003). Finally, all intracranial recordings in human subjects lack histological confirmation of the origin of the recorded activity, thus the electrode placement remains presumptive. However, postoperative imaging and MRI-based electrode localization in all of our patients was consistent with at least two contacts of the DBS electrode placed in the GPi.

The observed findings for the theta and the beta band are similar to previously described subthalamic LFP-MEG connectivity patterns from patients with Parkinson's disease (Hirschmann *et al.*, 2011; Litvak *et al.*, 2011*a*; Neumann *et al.*, 2014). Subcortico-cortical coherence with the temporal lobe has been described in these studies for the lower (yet alpha band) frequency range, whereas beta oscillations were primarily synchronized to sensorimotor regions. We describe a pallido-temporal network in the theta frequency range, which overlaps spatially with the hippocampus. The hippocampal theta rhythm is one of the most prominent oscillatory phenomena (Buzsaki and Draguhn, 2004) that has previously been described in MEG studies (Tesche, 1997; Tesche and Karhu, 2000*a*; Cornwell *et al.*, 2012), and recently further supported by evidence from parallel hippocampal LFP-MEG recordings that has given first-line evidence for the feasibility of recording human hippocampal theta rhythms with MEG (Dalal *et al.*, 2013). The hippocampus is anatomically interconnected with the pallidum via the nucleus accumbens and proposed to be simultaneously activated during learning and integration of limbic information on sensorimotor output (Thierry *et al.*, 2000; Packard and Knowlton, 2002). Theta synchronization has been hypothesized to allow encoding of new information in hippocampo-cortical feedback loops (Klimesch, 1999), and theta band coherence between the hippocampus and the basal ganglia was previously described in rats, where the striatum has been reported to be driving information flow (DeCoteau *et al.*, 2007). Thus, the hippocampus is a tempting candidate as a source for the described mid-temporal oscillatory theta network. However, given the low spatial resolution of the method and the relatively small size of the hippocampus and the larger extent of the described source, we propose a hippocampal network as one potential explanation of our findings, while keeping in mind that further studies would be needed to confirm this hypothesis through functional modulations of this oscillatory circuit to also elucidate its functional significance in dystonia.

The role of beta oscillatory activity in the cortico-basal ganglia circuit is comparatively much more studied, and beta network alterations have been reported in a variety of studies (Pfurtscheller and Aranibar, 1977; Pfurtscheller and Lopes da Silva, 1999; Kühn *et al.*, 2004, 2008*a*, *b*; Lalo *et al.*, 2007; Ray *et al.*, 2008; Hirschmann *et al.*, 2011; Litvak *et al.*, 2011*a*; Brücke *et al.*, 2012; Alegre *et al.*, 2013). A suppression of beta band activity has frequently been reported during motor tasks in the motor cortex (Pfurtscheller and Aranibar, 1977; Pfurtscheller and Lopes da Silva, 1999; Lalo *et al.*, 2007), GPi (Brücke *et al.*, 2008, 2012; Singh *et al.*, 2011*a*, *b*; Herrojo Ruiz *et al.*, 2014), the subthalamic nucleus (Kühn *et al.*, 2004; Litvak *et al.*, 2012; Alegre *et al.*, 2013) and the motor thalamus (Paradiso *et al*, 2004; Kempf *et al.*, 2009; Brücke *et al.*, 2013). Thus, beta activity in the cortico-basal ganglia loops has been widely associated with movement initiation and termination in motor control (Jenkinson and Brown, 2011; Brittain and Brown, 2014). Stimulation of the motor cortex in the beta frequency range has been shown to slow movements, which is first-line evidence for a causal influence of this network activity on motor performance (Pogosyan *et al.*, 2009; Joundi *et al.*, 2012). More specifically, beta circuit synchronization may promote the status quo or generally tonic activity (Engel and Fries, 2010; Jenkinson and Brown, 2011), and premovement beta desynchronization could signal the likelihood that a new voluntary action will need to be performed (Jenkinson and Brown, 2011). Altered movement-related beta band desynchronization over motor cortical areas (Toro *et al.*, 2000), and abnormal beta band functional connectivity across premotor–motor areas during movement (Jin *et al.*, 2011) provides further evidence for motor cortical involvement in dystonia linked to alterations in beta band oscillatory activity. Our study demonstrates a cortico-pallidal beta network at rest that is spatially restricted to the sensorimotor area, and thus gives a framework for functional interactions of cortico-pallidal beta signalling in the cortex-basal ganglia feedback loops for motor control. Abnormal movement-related beta signalling may occur in the described motor network leading to impaired motor learning in dystonia. The oscillatory driving of information flow by the motor cortex could either be indirect via a corticostriatal connection or monosynaptic through the recently described super-direct pathway that links Area 4 and 6 with the internal pallidum (Milardi *et al.*, 2014). It is interesting to note that both alpha and beta oscillatory activity is suppressed before and during movement, but demonstrate topographical and temporal differences that implicate these rhythms as functionally distinct (Pfurtscheller and Lopes da Silva, 1999). PET studies have revealed remote effects of pallidal DBS on premotor and motor areas at rest (Detante *et al.*, 2004) and during movement (Kumar *et al.*, 1999). Moreover, neurophysiological parameters of motor cortex excitability, intracortical inhibition and induced plasticity tend to normalize in parallel with alleviation of dystonic symptoms after chronic DBS, as revealed with transcranial magnetic stimulation (Kühn *et al.*, 2003; Tisch *et al.*, 2006; Ruge *et al.*, 2011*a*, *b*). Modulation of cortical activity patterns may be facilitated by a functional reorganization through

DBS-related modulation of oscillatory long range network synchronization.

Although there is a vast amount of literature that has established MEG recordings for the characterization of cortical surface activity, fewer studies have shown activity from deeper brain structures such as the cerebellum. Nevertheless, cerebellar signals picked up by MEG have been reported in association with somatosensory stimulation (Tesche and Karhu, 1997, 2000*b*; Stancak *et al.*, 2011), motor tasks (Jousmaki *et al.*, 1996; Gross *et al.*, 2002; Pollok *et al.*, 2005; Jerbi *et al.*, 2007; Bourguignon *et al.*, 2012), saccades (Ioannides *et al.*, 2005) and pathological conditions, such as epileptic seizures (Mohamed *et al.*, 2011), parkinsonian tremor (Timmermann *et al.*, 2003; Pollok *et al.*, 2009) and in patients with writer's cramp during writing (Butz *et al.*, 2006). Our results extend these findings, suggesting that the cerebellum is interconnected with the internal pallidum through 7–13 Hz alpha band oscillations. A cerebello-thalamo-cortical network at ~10 Hz has been proposed to reflect a fundamental network for the synchronization of spatially separated motor areas for the maintenance of intermittent motor control (Welsh *et al.*, 1995; Gross *et al.*, 2002). Alteration of functional connectivity in cerebellar pathways is consistent with recent findings of functional and structural abnormalities in patients with different types of dystonia; for example, a cerebellar hypermetabolism found during rest (Eidelberg *et al.*, 1998) and with pallidal DBS using PET (Detante *et al.*, 2004), as well as a reduced cerebellar activation during motor execution (Carbon *et al.*, 2008; Argyelan *et al.*, 2009; Blood, 2013). While there is extensive evidence that the cerebellum and the basal ganglia are interconnected (Bostan *et al.*, 2010, 2013; Bostan and Strick, 2010; Kipping *et al.*, 2013), no direct anatomical connection between the internal pallidum and the cerebellum has been described, making a monosynaptic oscillatory connection that could explain our findings highly unlikely. However, a close connection between the GPi and cerebellum via the red nucleus (a relay nucleus for afferent connections to the cerebellum and in the cerebello-thalamic circuit) has previously been reported and implicated in dystonia (Blood, 2013). More specifically, alterations in structural white matter connectivity between the internal pallidum and the red nucleus have been reported in a diffusion tensor imaging study of patients with dystonia (Argyelan *et al.*, 2009; Blood *et al.*, 2012). A pathway via the red nucleus offers a feasible explanation for the pallido-cerebellar oscillatory connectivity presented in this study, which would be corroborated by the pallidal drive of information flow found in the directionality analysis. Alterations in structural connectivity are likely associated with alterations in functional connectivity, which could lead to a disease-specific signature of oscillatory pallido-cerebellar network activity. The inverse correlation between pallido-cerebellar coupling and dystonic symptom severity suggests that alpha band connectivity is necessary for physiological motor and posture maintenance, and is disturbed in dystonia. Similar to the reported low frequency peaks in our patients, previous studies have shown that dystonia patients show increased low frequency (4–12 Hz) synchrony in the pallidal LFP signature (Silberstein *et al.*, 2003; Liu *et al.*, 2008) that drives (Sharott *et al.*, 2008) and correlates (Chen *et al.*, 2006) with dystonic muscle activity and is suppressed by DBS (Barow *et al.*, 2014). Whether increased pallidal low frequency synchronization is related to the loss of pallido-cerebellar coupling, e.g. as a compensatory mechanism, or may disrupt cortico-pallidal coupling itself will have to be investigated in future studies. Sensorimotor cortico-pallidal low frequency coherence was not correlated with dystonic symptoms at rest in our patients. Future studies should explore frequency-specific network changes during movement to further define its pathophysiological role for abnormal movement generation. In this context, it is of note that reduced cerebello-thalamic fibre tract integrity has been revealed in patients with dystonia (Argyelan *et al.*, 2009; Carbon *et al.*, 2011). Here, a larger amount of cerebellar outflow tract disruption was related not only to the occurrence of dystonic symptoms but associated with increased motor cortical activation at rest and during movement, suggesting interdependent network modulation (Carbon *et al.*, 2011). Similarly, increased cerebello-motor cortical functional connectivity has been described as a potential compensatory mechanism in patients with writer's cramp using functional MRI that was progressively reduced with larger symptom severity, indicating symptom-related neuroplastic compensatory network changes in dystonia (Dresel *et al.*, 2014). Moreover, recent findings suggest that modulation of cerebellar output by continuous theta burst transcranial magnetic stimulation modulates motor cortex activity via cerebello-pallido-thalamo-cortical pathways and thereby may improve dystonia or levodopa-induced dyskinesia in Parkinson's disease (Koch *et al.*, 2009). It could be speculated that theta burst stimulation may either enhance cerebello-pallidal low frequency connectivity or may transiently disrupt abnormal pallidal oscillations, thus leading to short-term improvement in dystonic symptoms. If so, cerebellar transcranial magnetic stimulation could be of potential interest to define optimal DBS candidates in the future.

In conclusion, we have demonstrated that cortico-pallidal circuits are interconnected via spatially and spectrally distinct oscillatory networks. Our findings suggest the existence of three segregated circuits that show a disease-related pattern. Deep brain stimulation may interfere with these networks, and could modulate abnormal motor circuit signalling in dystonia.

Acknowledgements

We would like to thank Lutz Trahms (Physikalisch Technische Bundesanstalt, Berlin, Germany), Vadim Nikulin (Neurophysics Group, Department of Neurology,

Charité - University Medicine Berlin, Germany) and Gabriel Curio (Neurophysics Group, Department of Neurology, Charité - University Medicine Berlin, Germany) for helpful discussions.

Funding

This work was supported by the German Federal Ministry of Education and Research (BMBF) project 'dystract'. W.J.N. was supported by a research grant by the German Society For Clinical Neurophysiology and Functional Imaging (DGKN). A.A.K. was supported by the German Research Foundation (DFG) grant KFO247.

Supplementary material

Supplementary material is available at *Brain* online.

References

Alegre M, Lopez-Azcarate J, Obeso I, Wilkinson L, Rodriguez-Oroz MC, Valencia M, et al. The subthalamic nucleus is involved in successful inhibition in the stop-signal task: a local field potential study in Parkinson's disease. Exp Neurol 2013; 239: 1–12

Argyelan M, Carbon M, Niethammer M, Ulug AM, Voss HU, Bressman SB, et al. Cerebellothalamocortical connectivity regulates penetrance in dystonia. J Neurosci 2009; 29: 9740–7.

Barow E, Neumann WJ, Brücke C, Huebl J, Horn A, Brown P, et al. Deep brain stimulation suppresses pallidal low frequency activity in patients with phasic dystonic movements. Brain 2014; 137 (Pt 11): 3012–24

Blood AJ. Imaging studies in focal dystonias: a systems level approach to studying a systems level disorder. Curr Neuropharmacol 2013; 11: 3–15.

Blood AJ, Kuster JK, Woodman SC, Kirlic N, Makhlouf ML, Multhaupt-Buell TJ, et al. Evidence for altered basal ganglia-brainstem connections in cervical dystonia. PLoS One 2012; 7: e31654.

Bostan AC, Dum RP, Strick PL. The basal ganglia communicate with the cerebellum. Proc Natl Acad Sci USA 2010; 107: 8452–6.

Bostan AC, Dum RP, Strick PL. Cerebellar networks with the cerebral cortex and basal ganglia. Trends Cogn Sci 2013; 17: 241–54.

Bostan AC, Strick PL. The cerebellum and basal ganglia are interconnected. Neuropsychol Rev 2010; 20: 261–70.

Bourguignon M, De Tiege X, de Beeck MO, Van Bogaert P, Goldman S, Jousmaki V, et al. Primary motor cortex and cerebellum are coupled with the kinematics of observed hand movements. Neuroimage 2012; 66c: 500–7.

Brittain JS, Brown P. Oscillations and the basal ganglia: motor control and beyond. Neuroimage 2014; 85 (Pt 2): 637–47.

Brovelli A, Ding M, Ledberg A, Chen Y, Nakamura R, Bressler SL. Beta oscillations in a large-scale sensorimotor cortical network: directional influences revealed by Granger causality. Proc Natl Acad Sci USA 2004; 101: 9849–54.

Brown P, Eusebio A. Paradoxes of functional neurosurgery: clues from basal ganglia recordings. Mov Disord 2008; 23: 12–20; quiz 158.

Brown P, Williams D. Basal ganglia local field potential activity: character and functional significance in the human. Clin Neurophysiol 2005; 116: 2510–19.

Brücke C, Bock A, Huebl J, Krauss JK, Schonecker T, Schneider GH, et al. Thalamic gamma oscillations correlate with reaction time in a Go/noGo task in patients with essential tremor. Neuroimage 2013; 75: 36–45.

Brücke C, Huebl J, Schonecker T, Neumann WJ, Yarrow K, Kupsch A, et al. Scaling of movement is related to pallidal gamma oscillations in patients with dystonia. J Neurosci 2012; 32: 1008–19.

Brücke C, Kempf F, Kupsch A, Schneider GH, Krauss JK, Aziz T, et al. Movement-related synchronization of gamma activity is lateralized in patients with dystonia. Eur J Neurosci France 2008; 27: 2322–9.

Butz M, Timmermann L, Gross J, Pollok B, Dirks M, Hefter H, et al. Oscillatory coupling in writing and writer's cramp. J Physiol Paris 2006; 99: 14–20.

Buzsaki G, Draguhn A. Neuronal oscillations in cortical networks. Science 2004; 304: 1926–9.

Carbon M, Argyelan M, Ghilardi MF, Mattis P, Dhawan V, Bressman S, et al. Impaired sequence learning in dystonia mutation carriers: a genotypic effect. Brain 2011; 134 (Pt 5) 1416–27.

Carbon M, Ghilardi MF, Argyelan M, Dhawan V, Bressman SB, Eidelberg D. Increased cerebellar activation during sequence learning in DYT1 carriers: an equiperformance study. Brain 2008; 131 (Pt 1): 146–54.

Ceballos-Baumann AO, Passingham RE, Warner T, Playford ED, Marsden CD, Brooks DJ. Overactive prefrontal and underactive motor cortical areas in idiopathic dystonia. Ann Neurol 1995; 37: 363–72.

Chen CC, Kühn AA, Hoffmann KT, Kupsch A, Schneider GH, Trottenberg T, et al. Oscillatory pallidal local field potential activity correlates with involuntary EMG in dystonia. Neurology 2006; 66: 418–20.

Cornwell BR, Arkin N, Overstreet C, Carver FW, Grillon C. Distinct contributions of human hippocampal theta to spatial cognition and anxiety. Hippocampus 2012; 22: 1848–59.

Dalal S, Jerbi K, Bertrand O, Adam C, Ducorps A, Schwartz D, et al. Simultaneous MEG-intracranial EEG: New insights into the ability of MEG to capture oscillatory modulations in the neocortex and the hippocampus. Epilepsy and Behavior 2013; 28: 288–290. doi:10.1016/j.yebeh.2013.03.012.

DeCoteau WE, Thorn C, Gibson DJ, Courtemanche R, Mitra P, Kubota Y, et al. Learning-related coordination of striatal and hippocampal theta rhythms during acquisition of a procedural maze task. Proc Natl Acad Sci USA 2007; 104: 5644–9.

Detante O, Vercueil L, Thobois S, Broussolle E, Costes N, Lavenne F, et al. Globus pallidus internus stimulation in primary generalized dystonia: a H215O PET study. Brain 2004; 127 (Pt 8): 1899–908.

Dresel C, Li Y, Wilzeck V, Castrop F, Zimmer C, Haslinger B. Multiple changes of functional connectivity between sensorimotor areas in focal hand dystonia. J Neurol Neurosurg Psychiatry 2014; 85: 1245–52.

Eidelberg D, Moeller JR, Antonini A, Kazumata K, Nakamura T, Dhawan V, et al. Functional brain networks in DYT1 dystonia. Ann Neurol 1998; 44: 303–12.

Engel AK, Fries P. Beta-band oscillations–signalling the status quo? Curr Opin Neurobiol 2010; 20: 156–65.

Fahn S. Concept and classification of dystonia. Adv Neurol 1988; 50: 1–8.

Frazier JA, Chiu S, Breeze JL, Makris N, Lange N, Kennedy DN, et al. Structural brain magnetic resonance imaging of limbic and thalamic volumes in pediatric bipolar disorder [Internet]. Am J Psychiatry 2005; 162: 1256–65.

Friston KJ, Holmes AP, Worsley KJ, Poline JP, Frith CD, Frackowiak RSJ. Statistical parametric maps in functional imaging: A general linear approach. Human Brain Mapping 1994; 2: 189–210.

Gross J, Kujala J, Hamalainen M, Timmermann L, Schnitzler A, Salmelin R. Dynamic imaging of coherent sources: studying neural interactions in the human brain. Proc Natl Acad Sci USA 2001; 98: 694–9.

Gross J, Timmermann L, Kujala J, Dirks M, Schmitz F, Salmelin R, et al. The neural basis of intermittent motor control in humans. Proc Natl Acad Sci USA 2002; 99: 2299–302.
Hallett M. Pathophysiology of dystonia. J Neural Transm 2006; Suppl: 485–8.
Hammond C, Bergman H, Brown P. Pathological synchronization in Parkinson's disease: networks, models and treatments. Trends Neurosci 2007; 30: 357–64.
Haufe S, Nikulin VV, Muller KR, Nolte G. A critical assessment of connectivity measures for EEG data: a simulation study. Neuroimage 2013; 64: 120–33.
Hendrix CM, Vitek JL. Toward a network model of dystonia. Ann NY Acad Sci 2012; 1265: 46–55.
Herrojo Ruiz M, Huebl J, Schonecker T, Kupsch A, Yarrow K, Krauss JK, et al. Involvement of human internal globus pallidus in the early modulation of cortical error-related activity. Cereb Cortex 2014; 24: 1502–17.
Hirschmann J, Hartmann CJ, Butz M, Hoogenboom N, Ozkurt TE, Elben S, et al. A direct relationship between oscillatory subthalamic nucleus-cortex coupling and rest tremor in Parkinson's disease. Brain 2013; 136 (Pt 12): 3659–70.
Hirschmann J, Özkurt TE, Butz M, Homburger M, Elben S, Hartmann CJ, et al. Distinct oscillatory STN-cortical loops revealed by simultaneous MEG and local field potential recordings in patients with Parkinson's disease. Neuroimage 2011; 55: 1159–68.
Horn A, Kühn A. Lead-DBS: a toolbox for deep brain stimulation electrode localizations and visualizations. Neuroimage 2015; 107C: 127–35.
Ioannides AA, Fenwick PB, Liu L. Widely distributed magnetoencephalography spikes related to the planning and execution of human saccades. J Neurosci 2005; 25: 7950–67.
Jenkinson N, Brown P. New insights into the relationship between dopamine, beta oscillations and motor function. Trends Neurosci 2011; 34: 611–18.
Jerbi K, Lachaux JP, N'Diaye K, Pantazis D, Leahy RM, Garnero L, et al. Coherent neural representation of hand speed in humans revealed by MEG imaging. Proc Natl Acad Sci USA. 2007; 104: 7676–81.
Jin SH, Lin P, Auh S, Hallett M. Abnormal functional connectivity in focal hand dystonia: mutual information analysis in EEG. Mov Disord 2011; 26: 1274–81.
Joundi RA, Jenkinson N, Brittain JS, Aziz TZ, Brown P. Driving oscillatory activity in the human cortex enhances motor performance. Curr Biol 2012; 22: 403–7.
Jousmaki V, Hamalainen M, Hari R. Magnetic source imaging during a visually guided task. Neuroreport 1996; 7: 2961–4.
Kempf F, Brücke C, Salih F, Trottenberg T, Kupsch A, Schneider GH, et al. Gamma activity and reactivity in human thalamic local field potentials. Eur J Neurosci 2009; 29: 943–53.
Kipping JA, Grodd W, Kumar V, Taubert M, Villringer A, Margulies DS. Overlapping and parallel cerebello-cerebral networks contributing to sensorimotor control: an intrinsic functional connectivity study. Neuroimage 2013; 83: 837–48.
Klimesch W. EEG alpha and theta oscillations reflect cognitive and memory performance: a review and analysis. Brain Res Brain Res Rev 1999; 29: 169–95.
Koch G, Brusa L, Carrillo F, Lo Gerfo E, Torriero S, Oliveri M, et al. Cerebellar magnetic stimulation decreases levodopa-induced dyskinesias in Parkinson disease. Neurology 2009; 73: 113–19.
Kühn AA, Brücke C, Schneider GH, Trottenberg T, Kivi A, Kupsch A, et al. Increased beta activity in dystonia patients after drug-induced dopamine deficiency. Exp Neurol 2008a; 214: 140–3.
Kühn AA, Kempf F, Brücke C, Gaynor Doyle L, Martinez-Torres I, Pogosyan A, et al. High-frequency stimulation of the subthalamic nucleus suppresses oscillatory beta activity in patients with Parkinson's disease in parallel with improvement in motor performance. J Neurosci 2008b; 28: 6165–73.
Kühn AA, Meyer BU, Trottenberg T, Brandt SA, Schneider GH, Kupsch A. Modulation of motor cortex excitability by pallidal stimulation in patients with severe dystonia. Neurology 2003; 60: 768–74.
Kühn AA, Williams D, Kupsch A, Limousin P, Hariz M, Schneider GH, et al. Event-related beta desynchronization in human subthalamic nucleus correlates with motor performance. Brain 2004; 127 (Pt 4): 735–46.
Kumar R, Dagher A, Hutchison WD, Lang AE, Lozano AM. Globus pallidus deep brain stimulation for generalized dystonia: clinical and PET investigation. Neurology 1999; 53: 871–4.
Kupsch A, Benecke R, Müller J, Trottenberg T, Schneider GH, Poewe W, et al. Pallidal deep-brain stimulation in primary generalized or segmental dystonia. N Engl J Med 2006; 355: 1978–90.
Lalo E, Gilbertson T, Doyle L, Di Lazzaro V, Cioni B, Brown P. Phasic increases in cortical beta activity are associated with alterations in sensory processing in the human. Exp Brain Res 2007; 177: 137–45.
Laufs H, Krakow K, Sterzer P, Eger E, Beyerle A, Salek-Haddadi A, et al. Electroencephalographic signatures of attentional and cognitive default modes in spontaneous brain activity fluctuations at rest. Proc Natl Acad Sci USA 2003; 100: 11053–8.
Lehericy S, Tijssen MA, Vidailhet M, Kaji R, Meunier S. The anatomical basis of dystonia: current view using neuroimaging. Mov Disord 2013; 28: 944–57.
Litvak V, Eusebio A, Jha A, Oostenveld R, Barnes G, Foltynie T, et al. Movement-related changes in local and long-range synchronization in Parkinson's disease revealed by simultaneous magnetoencephalography and intracranial recordings. J Neurosci. 2012; 32(31): 10541–53.
Litvak V, Eusebio A, Jha A, Oostenveld R, Barnes GR, Penny WD, et al. Optimized beamforming for simultaneous MEG and intracranial local field potential recordings in deep brain stimulation patients. Neuroimage. 2010; 50(4): 1578–88.
Litvak V, Jha A, Eusebio A, Oostenveld R, Foltynie T, Limousin P, et al. Resting oscillatory cortico-subthalamic connectivity in patients with Parkinson's disease. Brain 2011a; 134 (Pt 2): 359–74.
Litvak V, Mattout J, Kiebel S, Phillips C, Henson R, Kilner J, et al. EEG and MEG data analysis in SPM8. Comput Intell Neurosci 2011b; 2011: 852961.
Liu X, Wang S, Yianni J, Nandi D, Bain PG, Gregory R, et al. The sensory and motor representation of synchronized oscillations in the globus pallidus in patients with primary dystonia. Brain 2008; 131 (Pt 6): 1562–73.
Mattout J, Henson RN, Friston KJ. Canonical source reconstruction for MEG. Comput Intell Neurosci 2007: 67613.
McIntyre CC, Hahn PJ. Network perspectives on the mechanisms of deep brain stimulation. Neurobiol Dis 2010; 38: 329–37.
Milardi D, Gaeta M, Marino S, Arrigo A, Vaccarino G, Mormina E, et al. Basal ganglia network by constrained spherical deconvolution: a possible cortico-pallidal pathway? [Internet]. Mov Disord 2014. Available from: http://dx.doi.org/10.1002/mds.25995
Mohamed IS, Otsubo H, Ferrari P, Ochi A, Snead OC, Cheyne D. Neuromagnetic cerebellar activation during seizures arising from the motor cortex. Epilepsy Res 2011; 96: 283–7.
Neumann W-J, Bock A, Jha A, Huebl J, Brücke C, Schneider G-H, et al. Kortiko-subthalamische oszillatorische Konnektivität in Patienten mit idiopathischem Parkinson-Syndrom DGKN. Berlin: Klin Neurophysiol; 2014. p. 45.
Nolte G. The magnetic lead field theorem in the quasi-static approximation and its use for magnetoencephalography forward calculation in realistic volume conductors. Phys Med Biol 2003; 48: 3637–52.
Oostenveld R, Fries P, Maris E, Schoffelen JM. FieldTrip: open source software for advanced analysis of MEG, EEG, and invasive electrophysiological data. Comput Intell Neurosci 2011; 2011: 156869.
Ostrem JL, Starr PA. Treatment of dystonia with deep brain stimulation. Neurotherapeutics 2008; 5: 320–30.

Oswal A, Brown P, Litvak V. Movement related dynamics of subthalmo-cortical alpha connectivity in Parkinson's disease. Neuroimage 2013; 70: 132–42.

Packard MG, Knowlton BJ. Learning and memory functions of the Basal Ganglia. Annu Rev Neurosci 2002; 25: 563–93.

Paradiso G, Cunic D, Saint-Cyr J, Hoque T, Lozano A, Lang A, et al. Involvement of human thalamus in the preparation of self-paced movement. Brain 2004; 127: 2717–31.

Pfurtscheller G, Aranibar A. Event-related cortical desynchronization detected by power measurements of scalp EEG. Electroencephalogr Clin Neurophysiol 1977; 42: 817–26.

Pfurtscheller G, Lopes da Silva FH. Event-related EEG/MEG synchronization and desynchronization: basic principles. Clin Neurophysiol 1999; 110: 1842–57.

Pogosyan A, Gaynor LD, Eusebio A, Brown P. Boosting cortical activity at Beta-band frequencies slows movement in humans. Curr Biol 2009; 19: 1637–41.

Pollok B, Makhloufi H, Butz M, Gross J, Timmermann L, Wojtecki L, et al. Levodopa affects functional brain networks in Parkinsonian resting tremor. Mov Disord 2009; 24: 91–8.

Pollok B, Sudmeyer M, Gross J, Schnitzler A. The oscillatory network of simple repetitive bimanual movements. Brain Res Cogn Brain Res 2005; 25: 300–11.

Prodoehl J, Yu H, Little DM, Abraham I, Vaillancourt DE. Region of interest template for the human basal ganglia: comparing EPI and standardized space approaches [Internet]. Neuroimage 2008; 39: 956–65.

Quartarone A, Hallett M. Emerging concepts in the physiological basis of dystonia. Mov Disord 2013; 28: 958–67.

Ray NJ, Jenkinson N, Wang S, Holland P, Brittain JS, Joint C, et al. Local field potential beta activity in the subthalamic nucleus of patients with Parkinson's disease is associated with improvements in bradykinesia after dopamine and deep brain stimulation. Exp Neurol 2008; 213: 108–13.

Ruge D, Cif L, Limousin P, Gonzalez V, Vasques X, Hariz MI, et al. Shaping reversibility? Long-term deep brain stimulation in dystonia: the relationship between effects on electrophysiology and clinical symptoms. Brain 2011a; 134 (Pt 7): 2106–15.

Ruge D, Tisch S, Hariz MI, Zrinzo L, Bhatia KP, Quinn NP, et al. Deep brain stimulation effects in dystonia: time course of electrophysiological changes in early treatment. Mov Disord 2011b; 26: 1913–21.

Sharott A, Grosse P, Kühn AA, Salih F, Engel AK, Kupsch A, et al. Is the synchronization between pallidal and muscle activity in primary dystonia due to peripheral afferance or a motor drive? Brain 2008; 131 (Pt 2): 473–84.

Silberstein P, Kühn AA, Kupsch A, Trottenberg T, Krauss JK, Wohrle JC, et al. Patterning of globus pallidus local field potentials differs between Parkinson's disease and dystonia. Brain 2003; 126 (Pt 12): 2597–608.

Singh A, Kammermeier S, Plate A, Mehrkens JH, Ilmberger J, Botzel K. Pattern of local field potential activity in the globus pallidus internum of dystonic patients during walking on a treadmill. Exp Neurol. 2011a; 232: 162–7.

Singh A, Levin J, Mehrkens JH, Botzel K. Alpha frequency modulation in the human basal ganglia is dependent on motor task. Eur J Neurosci 2011b; 33: 960–7.

Stancak A, Alghamdi J, Nurmikko TJ. Cortical activation changes during repeated laser stimulation: a magnetoencephalographic study. PLoS One 2011; 6: e19744.

Tesche CD. Non-invasive detection of ongoing neuronal population activity in normal human hippocampus. Brain Res 1997; 749: 53–60.

Tesche CD, Karhu J. Somatosensory evoked magnetic fields arising from sources in the human cerebellum. Brain Res 1997; 744: 23–31.

Tesche CD, Karhu J. Theta oscillations index human hippocampal activation during a working memory task. Proc Natl Acad Sci USA 2000a; 97: 919–24.

Tesche CD, Karhu JJ. Anticipatory cerebellar responses during somatosensory omission in man. Hum Brain Mapp 2000b; 9: 119–42.

Thierry AM, Gioanni Y, Degenetais E, Glowinski J. Hippocampo-prefrontal cortex pathway: anatomical and electrophysiological characteristics. Hippocampus 2000; 10: 411–19.

Thomson DJ. Spectrum estimation and harmonic analysis. Proc IEEE 1982; 70: 1055–96.

Timmermann L, Gross J, Dirks M, Volkmann J, Freund HJ, Schnitzler A. The cerebral oscillatory network of parkinsonian resting tremor. Brain 2003; 126 (Pt 1): 199–212.

Tisch S, Limousin P, Rothwell JC, Asselman P, Zrinzo L, Jahanshahi M, et al. Changes in forearm reciprocal inhibition following pallidal stimulation for dystonia. Neurology 2006; 66: 1091–3.

Toro C, Deuschl G, Hallett M. Movement-related electroencephalographic desynchronization in patients with hand cramps: evidence for motor cortical involvement in focal dystonia. Ann Neurol 2000; 47: 456–61.

Van Veen BD, van Drongelen W, Yuchtman M, Suzuki A. Localization of brain electrical activity via linearly constrained minimum variance spatial filtering. IEEE Trans Biomed Eng 1997; 44: 867–80.

Vidailhet M, Dupel C, Lehericy S, Remy P, Dormont D, Serdaru M, et al. Dopaminergic dysfunction in midbrain dystonia: anatomoclinical study using 3-dimensional magnetic resonance imaging and fluorodopa F 18 positron emission tomography [Internet]. Arch Neurol 1999; 56: 982–9.

Vidailhet M, Grabli D, Roze E. Pathophysiology of dystonia. Curr Opin Neurol 2009; 22: 406–13.

Vidailhet M, Vercueil L, Houeto JL, Krystkowiak P, Benabid AL, Cornu P, et al. Bilateral deep-brain stimulation of the globus pallidus in primary generalized dystonia. N Engl J Med 2005; 352: 459–67.

Vidailhet M, Vercueil L, Houeto JL, Krystkowiak P, Lagrange C, Yelnik J, et al. Bilateral, pallidal, deep-brain stimulation in primary generalised dystonia: a prospective 3 year follow-up study. Lancet Neurol 2007; 6: 223–9.

Volkmann J, Mueller J, Deuschl G, Kühn AA, Krauss JK, Poewe W, et al. Pallidal neurostimulation in patients with medication-refractory cervical dystonia: a randomised, sham-controlled trial. Lancet Neurol 2014; 13: 875–84.

Volkmann J, Wolters A, Kupsch A, Muller J, Kühn AA, Schneider GH, et al. Pallidal deep brain stimulation in patients with primary generalised or segmental dystonia: 5-year follow-up of a randomised trial. Lancet Neurol 2012; 11: 1029–38.

Welsh JP, Lang EJ, Suglhara I, Llinas R. Dynamic organization of motor control within the olivocerebellar system. Nature 1995; 374: 453–7.

Williams D, Tijssen M, Van Bruggen G, Bosch A, Insola A, Di Lazzaro V, et al. Dopamine-dependent changes in the functional connectivity between basal ganglia and cerebral cortex in humans. Brain 2002; 125 (Pt 7): 1558–69.